Electronic viscosity and energy relaxation in neutral graphene

Vanessa Gall [1,2] Boris N. Narozhny [2,3] and Igor V. Gornyi [1,2,4]

[1]*Institute for Quantum Materials and Technologies, Karlsruhe Institute of Technology, 76021 Karlsruhe, Germany*
[2]*Institut für Theorie der Kondensierten Materie, Karlsruhe Institute of Technology, 76128 Karlsruhe, Germany*
[3]*National Research Nuclear University MEPhI (Moscow Engineering Physics Institute), 115409 Moscow, Russia*
[4]*Ioffe Institute, 194021 St. Petersburg, Russia*

We explore hydrodynamics of Dirac fermions in neutral graphene in the Corbino geometry. In the absence of a magnetic field, the bulk Ohmic charge flow and the hydrodynamic energy flow are decoupled. However, the energy flow does affect the overall resistance of the system through viscous dissipation and energy relaxation that has to be compensated by the work done by the current source. Solving the hydrodynamic equations, we find that local temperature and electric potential are discontinuous at the interfaces with the leads as well as the device resistance and argue that this makes Corbino geometry a feasible choice for an experimental observation of the Dirac fluid.

Quantum dynamics of charge carriers is one of the most important research directions in condensed matter physics. In many materials, transport properties can be successfully described under the assumption of weak electron-electron interaction allowing for free-electron theories [1]. An extension of this approach to strongly correlated systems remains a major unsolved problem. The advent of "ultraclean" materials poses new challenges, especially if the electronic system is nondegenerate. At high temperatures, such systems may exhibit signatures of a collective motion of charge carriers resembling the hydrodynamic flow of a viscous fluid [2–14].

Electronic viscosity has been discussed theoretically for a long time [15–20] but became the subject of dedicated experiments [2,9] only recently, after ultraclean materials became available. Up until now, most experimental efforts have focused on graphene [2–11], where the hydrodynamic regime is apparently easier to achieve [21–23]. Viscous effects manifest themselves in nonuniform flows. In the common "linear" geometry (channels, wires, Hall bars, etc.) this occurs in "narrow" samples where the typical length scale associated with viscosity is of the same order as the channel width [24–28]. In contrast, in the "circular" Corbino geometry (see Fig. 1), the electric current is nonuniform even in the simplest Drude picture (in the absence of a magnetic field, $j \propto e_r/|r|$, where $e_r = r/|r|$) making it an excellent platform to measure electronic viscosity [29–32]. In the last year, electronic hydrodynamics in the Corbino geometry has been studied both experimentally [33] and theoretically [34–37].

In this paper we address the "Dirac fluid" [3,9] (the hydrodynamic flow of charge carriers in neutral graphene) in the Corbino geometry. Unlike doped graphene, where degenerate, Fermi-liquid-like electrons may be described by the Navier-Stokes equation with a weak damping term due to disorder [16,21,24], the two-band physics of neutral graphene leads to unconventional hydrodynamics [22,38]. In the hydrodynamic

approach any macroscopic current can be expressed as a product of the corresponding density and hydrodynamic velocity u (up to dissipative corrections); for example, the electric and energy current densities are $j = nu$ and $j_E = n_E u$, respectively. In the degenerate regime the charge and energy densities are proportional to each other (to the leading approximation in thermal equilibrium $n_E = 2\mu n/3$, where μ is the chemical potential), and the two currents are equivalent [39]. In contrast, the equilibrium charge density vanishes at charge neutrality, $n(\mu = 0) = 0$, while the energy density remains finite. The two currents "decouple": The energy current remains "hydrodynamic," and the charge current is completely determined by the dissipative correction δj.

Electronic transport at charge neutrality has been the subject of intensive research [9,25–28,39–47] leading to general consensus on the basic result: In the absence of a magnetic field, $B = 0$, the resistivity of neutral graphene is determined by the electron-electron interaction

$$R_0 = \frac{\pi}{2e^2 T \ln 2} \left(\frac{1}{\tau_{11}} + \frac{1}{\tau_{\mathrm{dis}}} \right) \xrightarrow{\tau_{\mathrm{dis}} \to \infty} \frac{1}{\sigma_Q}. \qquad (1)$$

Here, $\tau_{11} \propto \alpha_g^{-2} T^{-1}$ describes the appropriate electron-electron collision integral, and σ_Q is the "intrinsic" or "quantum" conductivity of graphene. Disorder scattering is characterized by the mean free time τ_{dis}, which is large under the assumptions of the hydrodynamic regime, $\tau_{\mathrm{dis}} \gg \tau_{11}$, and yields a negligible contribution to Eq. (1). Equation (1) describes the uniform bulk current and is independent of viscosity (i.e., in a channel [21,25,45,47]). In contrast, in the Corbino geometry the current flow is necessarily inhomogeneous, and hence viscous dissipation must be taken into account.

We envision the following experiment: A graphene sample (at charge neutrality) in the shape of an annulus is
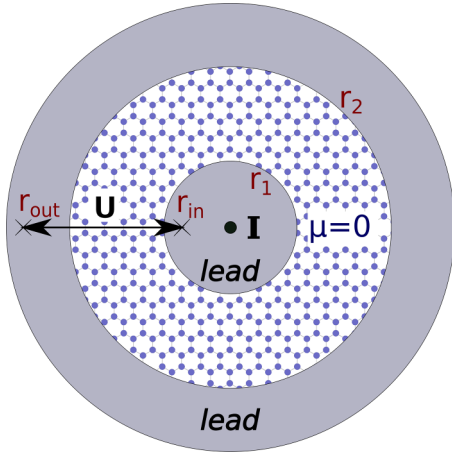
FIG. 1. Corbino geometry. The annulus-shaped sample of neutral graphene ($\mu = 0$) is placed between the the two leads: the inner circle of radius r_1 and the outer shell with inner radius r_2. A current I is injected through at the center point, and a voltage U is measured between electrodes placed at the inner and outer radii $r_{\rm in}$ and $r_{\rm out}$.

placed between the inner (a disk of radius r_1) and outer (a ring with inner radius r_2) metallic contacts (leads). For simplicity, we assume both leads to be of the same material, e.g., highly doped graphene with the same doping level. The electric current I is injected into the center of the inner lead preserving the rotational invariance (e.g., through a thin vertical wire attached to the center point) and spreads towards the outer lead, which for concreteness we assume to be grounded. The overall voltage drop U is measured between two points in the two leads (at the radii $r_{\rm in} < r_1$ and $r_{\rm out} > r_2$) yielding the device resistance, $R = U/I$, see Fig. 1. In most traditional measurements, the leads' resistance is minimal, while the contact resistance is important only in ballistic systems; see, e.g., Ref. [10]. Hence one may interpret the measured voltage drop in terms of the resistivity of the sample material. Here, we focus on the device resistance and show that in the hydrodynamic regime there is an additional contribution due to electronic viscosity and energy relaxation.

Charge flow through the Corbino disk can be described as follows. The injected current spreads through the inner lead according to Ohm's law and the continuity equation. In the stationary case, the latter determines the radial component of the current density, $j_r^{\rm in} = I/(2\pi e r)$. This defines the drift velocity $\boldsymbol{u}^{\rm in} = \boldsymbol{j}^{\rm in}/n^{\rm in}$ ($n^{\rm in}$ is the carrier density in the inner lead) and the energy current $\boldsymbol{j}_E^{\rm in} = n_E^{\rm in}\boldsymbol{u}^{\rm in}$. Reaching the interface, both currents continue to flow into the graphene sample. Charge conservation requires the radial component of the electric current to be continuous at the interface, $\delta\boldsymbol{j}(r_1) = \boldsymbol{j}^{\rm in}(r_1)$. Due to the continuity equation, the current density in graphene has the same functional form, $\delta j_r = I/(2\pi e r)$. Does this mean that the device resistance trivially follows if one knows the resistivity of graphene? The answer is "no," since the electrochemical potential is discontinuous at the interface! There are two mechanisms for the "jump" in the potential: (i) the usual Schottky contact resistance [43,48], and (ii) dissipation due to viscosity [32]

and energy relaxation [49]. Since the lost energy must come from the current source, both contribute to R.

In neutral graphene (at zero magnetic field), the energy current $\boldsymbol{j}_E = n_E \boldsymbol{u}$ is decoupled from the electric current $\boldsymbol{j} = \delta\boldsymbol{j}$, which means that, at charge neutrality, $\boldsymbol{u}$ is not responsible for any charge current in the sample. The flows in neutral graphene are described by the set of hydrodynamic equations derived in Refs. [38,45,49] and recently solved in Ref. [47] in the channel geometry. Within linear response, the static equations are

$$\nabla \cdot \delta \boldsymbol{j} = 0, \tag{2a}$$

$$n_I \nabla \cdot \boldsymbol{u} + \nabla \cdot \delta \boldsymbol{j}_I = -(12\ln 2/\pi^2)n_I\mu_I/(T\tau_R), \tag{2b}$$

$$\nabla \delta P = \eta \Delta \boldsymbol{u} - 3P\boldsymbol{u}/(v_g^2\tau_{\rm dis}), \tag{2c}$$

$$3P\nabla \cdot \boldsymbol{u} = -2\delta P/\tau_{RE}. \tag{2d}$$

Here, Eq. (2a) is the charge continuity equation; Eq. (2b) is the "imbalance" continuity equation [38,43] [μ_I is the imbalance chemical potential, $n_I = \pi T^2/(3v_g^2)$ is the equilibrium imbalance density, v_g is the band velocity in graphene, and τ_R is the recombination time]; Eq. (2c) is the linearized Navier-Stokes equation [38,47,50,51] with the shear viscosity η; and Eq. (2d) is the linearized "thermal transport" equation obtained from Eq. (S4d) of the Supplemental Material [52] for the "super-collision" relaxation model [49] (τ_{RE} is the energy relaxation time; for this model, $\tau_{RE} \lesssim \tau_R$).

Equilibrium thermodynamic quantities [the pressure $P = 3\zeta(3)T^3/(\pi v_g^2)$, enthalpy density $\mathcal{W}$, and energy density] are related by the "equation of state," $\mathcal{W} = 3P = 3n_E/2$. The dissipative corrections to the macroscopic currents are given by

$$\delta \boldsymbol{j} = \boldsymbol{E}/(eR_0), \tag{3a}$$

$$\delta \boldsymbol{j}_I = -\frac{2\gamma \ln 2}{\pi} T\tau_{\rm dis}\nabla\mu_I, \quad \gamma = \frac{\delta_I}{1 + \tau_{\rm dis}/(\delta_I\tau_{22})}, \tag{3b}$$

where $\tau_{22} \propto \alpha_g^{-2}T^{-1}$ describes a component of the collision integral that is qualitatively similar to, but quantitatively distinct from, τ_{11} and $\delta_I \approx 0.28$. At charge neutrality, the electric field $\boldsymbol{E}$ only enters the linear response equations through the dissipative correction [Eq. (3a)].

Equations (2a)–(2d), (3a), and (3b) should be solved for $\boldsymbol{u}$, $\delta\boldsymbol{j}$, $\delta\boldsymbol{j}_I$, $\boldsymbol{E}$, μ_I, and δP. We employ the boundary conditions that follow from the fact that we only have interfaces between the graphene sample and the leads in the Corbino geometry. Since there are no additional sinks or sources for charge, imbalance, and entropy at the interface, the corresponding currents (radial by symmetry) are conserved exactly (i.e., before employing hydrodynamic approximations) across the interface:

$$\delta\boldsymbol{j} = \boldsymbol{j}^L, \quad \delta\boldsymbol{j}_I = \boldsymbol{j}_I^L \simeq \boldsymbol{j}^L, \quad s\boldsymbol{u} = s^L\boldsymbol{u}^L$$

at both interfaces with leads (the superscript "L" denotes the quantities on the lead side; s and s_L are entropy densities). This does not fix the jump in the potential, which we discuss below.

Excluding δP from Eqs. (2c) and (2d), we find a second-order differential equation for $\boldsymbol{u}$

$$\eta'\Delta\boldsymbol{u} = 3P\boldsymbol{u}/(v_g^2\tau_{\rm dis}), \quad \eta' = \eta + 3P\tau_{RE}/2. \tag{4a}$$
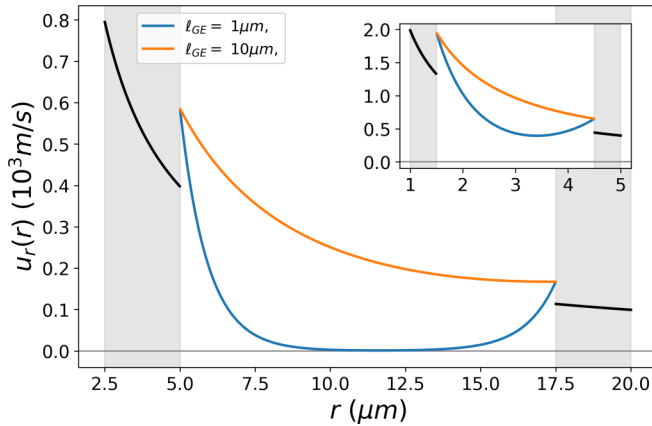
FIG. 2. Radial component of the hydrodynamic velocity u_r. Black curves show the drift velocity in the leads, $u_r^{\text{in(out)}} \propto 1/r$. Colored curves correspond to the solution, Eq. (4b), for the two indicated values of ℓ_{GE}. The results are plotted for the two cases of a large (main panel) and small (inset) device.

FIG. 3. Temperature distribution δT in the device. Colored curves correspond to the solution of the hydrodynamic equations for the indicated values of ℓ_{GE} and ℓ_R. The results are plotted for the two cases of a large (main panel) and small (inset) device. In the leads, $\delta T = 0$, shown by black lines.

Importantly, energy relaxation here renormalizes the value of viscosity, as the energy flow described by $\boldsymbol{u}$ becomes effectively compressible. It is also worth noticing that, in weakly disordered neutral graphene, the hydrodynamic velocity $\boldsymbol{u}$ vanishes in the homogeneous case. This is a consequence of charge-energy separation and energy relaxation described by Eq. (2d).

In the Corbino disk, the general solution for the radial component of the velocity has the form

$$u_r = a_1 I_1\left(\frac{r}{\ell_{GE}}\right) + a_2 K_1\left(\frac{r}{\ell_{GE}}\right), \quad \ell_{GE}^2 = \frac{v_g^2 \eta' \tau_{\text{dis}}}{3P}, \quad (4b)$$

where $I_1(z)$ and $K_1(z)$ are the Bessel functions. The coefficients a_1 and a_2 can be found using the continuity of the entropy current at the two interfaces (within linear response). The resulting behavior in shown in Fig. 2 (here we choose to show our results in graphical form since the analytic expressions are somewhat cumbersome [52]; quantitative calculations were performed for $T = 100$ K, $I = 1$ µA, and experimentally relevant values of the parameters were taken from Refs. [8–10,49]).

In the hydrodynamic regime, the electron-electron scattering time is the shortest scale in the problem; hence the spatial variation of $\boldsymbol{u}$ is determined by the energy relaxation. If $\ell_{GE} \ll r_{\text{out}} - r_{\text{in}}$, then the energy current injected from the leads decays in a (relatively small) boundary region while in the bulk of the sample $\boldsymbol{u} \to 0$. On the other hand, if ℓ_{GE} is of the same order as (or larger than) the system size, then u_r does not vanish and approaches the standard Corbino profile, $u_r \propto 1/r$. At each interface, u_r exhibits a jump due to the mismatch of the entropy densities in the sample and leads.

The nonequilibrium quantities δP and μ_I can now be found straightforwardly. The former follows directly from Eq. (2d) using the solution (4b), while the differential equation for the latter can be found by substituting Eq. (3b) into Eq. (2b) and using the solution (4b). The boundary conditions for δP and μ_I follow from the continuity equations for the charge and imbalance. The two quantities can be combined to determine
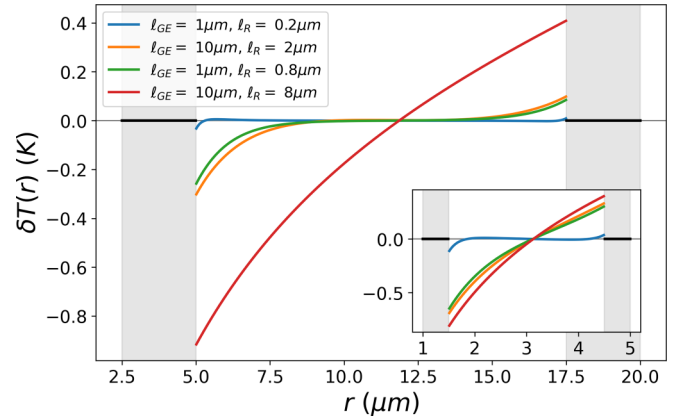
the nonequilibrium temperature variation,

$$\delta T = \frac{\pi v_g^2}{9T^2 \zeta(3)} \delta P - \frac{\pi^2}{27 \zeta(3)} \mu_I,$$

shown in Fig. 3. For a large sample ($\ell_{GE}, \ell_R \ll r_{\text{out}} - r_{\text{in}}$, $\ell_R^2 = \gamma v_g^2 \tau_{\text{dis}} \tau_R / 2$), δT exhibits fast decay and vanishes in the bulk of the sample. For larger values of ℓ_{GE}, ℓ_R, energy relaxation is less effective, and the system exhibits an inhomogeneous temperature profile.

The obtained solutions completely describe the hydrodynamic energy flow in neutral graphene. Our remaining task is to find the behavior of the electrochemical potential at the two interfaces enabling us to determine R. The standard description of interfaces between metals or semiconductors [48] can be carried over to neutral graphene [43] in terms of the contact resistance. Typically, this is a manifestation of the difference of work functions of the two materials across the interface. In graphene, the contact resistance was recently measured in Ref. [10]; see also Refs. [33,53,54]. In the standard diffusive (or Ohmic) case, the contact resistance leads to a voltage drop that is small compared with the voltage drop in the bulk of the sample and can be ignored. In contrast, in the ballistic case there is almost no voltage drop in the bulk, such that most energy is dissipated at the contacts. Both scenarios neglect electron-electron interactions.

In the diffusive case, interactions lead to corrections to the bulk resistivity [55,56], and the contact resistance can still be ignored. In the ballistic case, electron-electron interaction may give rise to a "Knudsen-Poiseuille" crossover [16] and drive the electronic system to the hydrodynamic regime. While the Ohmic resistivity of the electronic fluid may remain small, the hydrodynamic flow possesses another channel for dissipation through viscosity [32]. At charge neutrality, this effect is subtle, since the electric current is decoupled from the hydrodynamic energy flow; see Eq. (3a). At the same time, both are induced by the current source providing the energy dissipated not only by Ohmic effects, but also by viscosity [32] and energy relaxation processes [49] that should be taken into account in the form of an additional voltage drop. Since

the voltage drop in the bulk of the sample is completely determined by Eq. (3a), the additional contribution takes the form of a jump in ϕ at the interface corresponding to an excess electric field induced in the thin Knudsen layer around the interface [32].

The magnitude of the jump in ϕ can be established by considering the flow of energy through the interface. Following the standard route [32,57], we consider the time derivative of the kinetic energy, $\mathcal{A} = \dot{\mathcal{E}}$, where $\mathcal{E}$ is obtained by integrating the energy density $n_E(\boldsymbol{u}) - n_E(0)$ over the volume. Working within linear response, we expand the latter to the leading order in the hydrodynamic velocity. Finding time derivatives from the equations of motion and using the continuity equation and partial integration, we then separate the "bulk" and "boundary" contributions, $\mathcal{A} = \mathcal{A}_{\text{bulk}} + \mathcal{A}_{\text{edge}}$. We interpret the former as the bulk dissipation, while $\mathcal{A}_{\text{edge}}$ includes the energy brought in (carried away) through the boundary by the incoming (outgoing) flow. In the stationary state $\dot{\mathcal{E}} = 0$, dissipation is balanced by the work done by the source. Assuming that no energy is accumulated at the interface, we find the corresponding boundary condition.

The specific form of the equations of motion depends on the choice of the material. Assuming that the leads' material is highly doped graphene, the equation of motion is the usual Ohm's law with the diffusion term [58] coming from the gradient of the stress-energy tensor [39]; here we include a viscous contribution due to disorder [59] and find [32] (omitting the continuous entropy flux)

$$\mathcal{A}_{\text{edge}}^{\text{lead}} = \int dS_\beta \left(u_\alpha^L \sigma'_{L;\alpha\beta} - u_\beta^L \delta P_L - e j_\beta^L \phi \right), \tag{5a}$$

where $\boldsymbol{j}^L = n_L \boldsymbol{u}^L$ is the current density, $\boldsymbol{u}^L$ is the drift velocity, δP_L is the nonequilibrium pressure, and σ'_L is the viscous stress tensor in the lead. The first two terms are the usual dissipative contributions to the energy flow across the boundary [57], and the last term is the Joule heat.

In neutral graphene, we obtain similar results from the Navier-Stokes equation, except that the Joule heat is now determined by $\delta \boldsymbol{j}$

$$\mathcal{A}_{\text{edge}}^{\text{sample}} = \int dS_\beta \left(u_\alpha \sigma'_{\alpha\beta} - u_\beta \delta P - e \delta j_\beta \phi \right). \tag{5b}$$

Equating the two contributions (5a) and (5b) and using the above solutions for the velocity and pressure, we find the jumps in the potential ϕ at the two interfaces. This allows us to determine ϕ everywhere in the device (see Fig. 4), as well as the device resistance.

The total resistance of the Corbino device is shown in Fig. 5. Neglecting hydrodynamic effects, we find the usual logarithmic dependence of R on the system size. Viscosity and energy relaxation provide an additional dissipation channel and hence increase R. Energy relaxation contributes to this increase since it dominates the hydrodynamic energy flow; see Eqs. (4a) and (4b). At the same time, the boundary condition for the electric potential, Eqs. (5a) and (5b), is determined by viscosity.

In this paper we have solved the hydrodynamic equations in neutral graphene. We have shown that despite the known decoupling of the Ohmic charge flow and hydrodynamic energy flow, in Corbino geometry the latter does
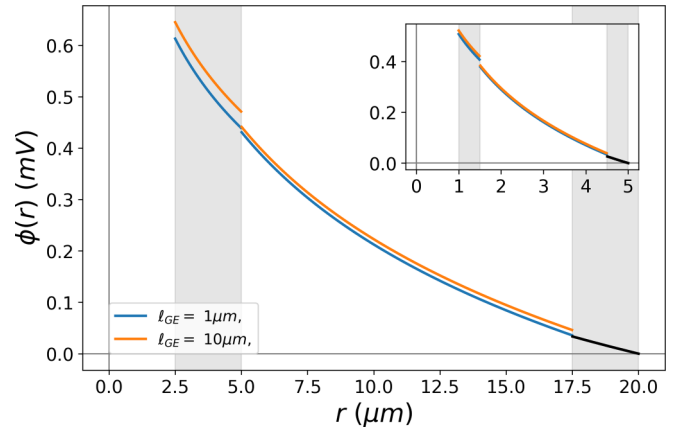
FIG. 4. Electrochemical potential (voltage drop) throughout the device. The resistive leads (shaded regions) show the Ohmic behavior. The jumps at the interfaces are due to dissipative effects (viscosity and energy relaxation) in the bulk of the sample.

affect the observable behavior leading to jumps in temperature (shown in Fig. 3) and the electric potential (see Fig. 4). The potential jump is distinct from the usual contact resistance insofar as it is a function of the system size. Both effects are observable using modern imaging techniques (the local temperature variation can be measured using the approach of Refs. [60–62], while measurements of the local potential are at the heart of the technique proposed in Refs. [10,63]). Hydrodynamics also affects the more conventional transport measurements through the size-dependent contribution to the device resistance (see Fig. 5).

Our results highlight several particular features of the Dirac fluid in neutral graphene. Firstly, the "linear response" currents (3a) and (3b) are independent of the temperature gradient due to exact particle-hole symmetry [43]. Secondly, in contrast to the case of doped graphene [32] *the Dirac fluid is compressible* even within linear response [due to energy relaxation; see Eq. (2d)]. Finally, the hydrodynamic flow in neutral graphene is the energy flow. Hence energy relaxation
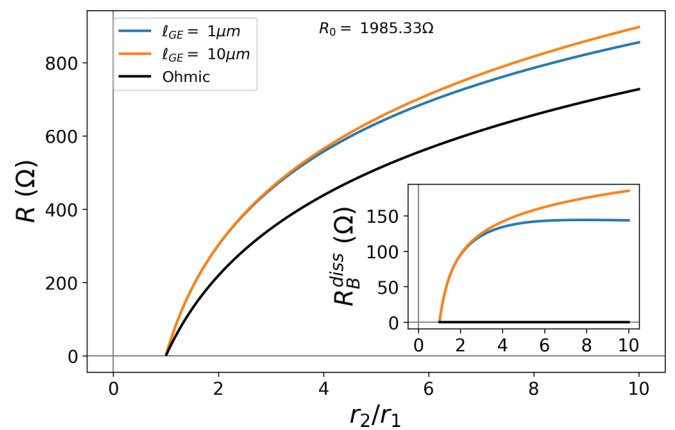
FIG. 5. Total resistance of the Corbino device for different values of ℓ_{GE} (here, $r_1 = 0.5\ \mu$m). Inset: Additional contribution to the resistance due to viscous dissipation.

effectively dominates over viscous effects [see Eqs. (4a) and (4b)], complicating experimental determination of η.

An external magnetic field is also known to couple the charge and energy flows in neutral graphene [38]. We expect that our theory will yield interesting results in the study of Corbino magnetoresistance [53]. Another extension of our theory is the study of thermoelectric phenomena, which is more interesting if one moves away from the neutrality point [35] (where the thermopower must vanish due to the exact particle-hole symmetry). Our results regarding both issues will be reported elsewhere.

[1] J. M. Ziman, *Principles of the Theory of Solids* (Cambridge University Press, Cambridge, 1965).

[2] D. A. Bandurin, I. Torre, R. Krishna Kumar, M. Ben Shalom, A. Tomadin, A. Principi, G. H. Auton, E. Khestanova, K. S. Novoselov, I. V. Grigorieva, L. A. Ponomarenko, A. K. Geim, and M. Polini, Science **351**, 1055 (2016).

[3] J. Crossno, J. K. Shi, K. Wang, X. Liu, A. Harzheim, A. Lucas, S. Sachdev, P. Kim, T. Taniguchi, K. Watanabe, T. A. Ohki, and K. C. Fong, Science **351**, 1058 (2016).

[4] R. Krishna Kumar, D. A. Bandurin, F. M. D. Pellegrino, Y. Cao, A. Principi, H. Guo, G. H. Auton, M. Ben Shalom, L. A. Ponomarenko, G. Falkovich, K. Watanabe, T. Taniguchi, I. V. Grigorieva, L. S. Levitov, M. Polini, and A. K. Geim, Nat. Phys. **13**, 1182 (2017).

[5] F. Ghahari, H.-Y. Xie, T. Taniguchi, K. Watanabe, M. S. Foster, and P. Kim, Phys. Rev. Lett. **116**, 136802 (2016).

[6] D. A. Bandurin, A. V. Shytov, L. S. Levitov, R. Krishna Kumar, A. I. Berdyugin, M. Ben Shalom, I. V. Grigorieva, A. K. Geim, and G. Falkovich, Nat. Commun. **9**, 4533 (2018).

[7] A. I. Berdyugin, S. G. Xu, F. M. D. Pellegrino, R. Krishna Kumar, A. Principi, I. Torre, M. B. Shalom, T. Taniguchi, K. Watanabe, I. V. Grigorieva, M. Polini, A. K. Geim, and D. A. Bandurin, Science **364**, 162 (2019).

[8] P. Gallagher, C.-S. Yang, T. Lyu, F. Tian, R. Kou, H. Zhang, K. Watanabe, T. Taniguchi, and F. Wang, Science **364**, 158 (2019).

[9] M. J. H. Ku, T. X. Zhou, Q. Li, Y. J. Shin, J. K. Shi, C. Burch, L. E. Anderson, A. T. Pierce, Y. Xie, A. Hamo, U. Vool, H. Zhang, F. Casola, T. Taniguchi, K. Watanabe, M. M. Fogler, P. Kim, A. Yacoby, and R. L. Walsworth, Nature (London) **583**, 537 (2020).

[10] J. A. Sulpizio, L. Ella, A. Rozen, J. Birkbeck, D. J. Perello, D. Dutta, M. Ben-Shalom, T. Taniguchi, K. Watanabe, T. Holder, R. Queiroz, A. Principi, A. Stern, T. Scaffidi, A. K. Geim, and S. Ilani, Nature (London) **576**, 75 (2019).

[11] A. Jenkins, S. Baumann, H. Zhou, S. A. Meynell, D. Yang, K. Watanabe, T. Taniguchi, A. Lucas, A. F. Young, and A. C. Bleszynski Jayich, Phys. Rev. Lett. **129**, 087701 (2022).

[12] P. J. W. Moll, P. Kushwaha, N. Nandi, B. Schmidt, and A. P. Mackenzie, Science **351**, 1061 (2016).

[13] B. A. Braem, F. M. D. Pellegrino, A. Principi, M. Röösli, C. Gold, S. Hennel, J. V. Koski, M. Berl, W. Dietsche, W. Wegscheider, M. Polini, T. Ihn, and K. Ensslin, Phys. Rev. B **98**, 241304(R) (2018).

[14] A. Jaoui, B. Fauqué, C. W. Rischau, A. Subedi, C. Fu, J. Gooth, N. Kumar, V. Süß, D. L. Maslov, C. Felser, and K. Behnia, npj Quantum Mater. **3**, 64 (2018).

[15] M. S. Steinberg, Phys. Rev. **109**, 1486 (1958).

[16] R. N. Gurzhi, Usp. Fiz. Nauk **94**, 689 (1968); [Sov. Phys.-Usp. **11**, 255 (1968)].

[17] B. Bradlyn, M. Goldstein, and N. Read, Phys. Rev. B **86**, 245309 (2012).

[18] P. S. Alekseev, Phys. Rev. Lett. **117**, 166601 (2016).

[19] T. Scaffidi, N. Nandi, B. Schmidt, A. P. Mackenzie, and J. E. Moore, Phys. Rev. Lett. **118**, 226601 (2017).

[20] B. N. Narozhny and M. Schütt, Phys. Rev. B **100**, 035125 (2019).

[21] A. Lucas and K. C. Fong, J. Phys.: Condens. Matter **30**, 053001 (2018).

[22] B. N. Narozhny, I. V. Gornyi, A. D. Mirlin, and J. Schmalian, Ann. Phys. (Berlin) **529**, 1700043 (2017).

[23] B. N. Narozhny, Riv. Nuovo Cimento **45**, 661 (2022).

[24] L. S. Levitov and G. Falkovich, Nat. Phys. **12**, 672 (2016).

[25] P. S. Alekseev, A. P. Dmitriev, I. V. Gornyi, V. Y. Kachorovskii, B. N. Narozhny, M. Schütt, and M. Titov, Phys. Rev. Lett. **114**, 156601 (2015).

[26] P. S. Alekseev, A. P. Dmitriev, I. V. Gornyi, V. Y. Kachorovskii, B. N. Narozhny, M. Schütt, and M. Titov, Phys. Rev. B **95**, 165410 (2017).

[27] P. S. Alekseev, A. P. Dmitriev, I. V. Gornyi, V. Y. Kachorovskii, B. N. Narozhny, and M. Titov, Phys. Rev. B **97**, 085109 (2018).

[28] P. S. Alekseev, A. P. Dmitriev, I. V. Gornyi, V. Y. Kachorovskii, B. N. Narozhny, and M. Titov, Phys. Rev. B **98**, 125111 (2018).

[29] O. M. Corbino, Nuovo Cimento **1**, 397 (1911).

[30] A. Tomadin, G. Vignale, and M. Polini, Phys. Rev. Lett. **113**, 235901 (2014).

[31] T. Holder, R. Queiroz, and A. Stern, Phys. Rev. Lett. **123**, 106801 (2019).

[32] M. Shavit, A. V. Shytov, and G. Falkovich, Phys. Rev. Lett. **123**, 026801 (2019).

[33] C. Kumar, J. Birkbeck, J. A. Sulpizio, D. Perello, T. Taniguchi, K. Watanabe, O. Reuven, T. Scaffidi, A. Stern, A. K. Geim, and S. Ilani, Nature (London) **609**, 276 (2022).

[34] A. Hui, V. Oganesyan, and E.-A. Kim, Phys. Rev. B **103**, 235152 (2021).

[35] S. Li, A. Levchenko, and A. V. Andreev, Phys. Rev. B **105**, 125302 (2022).

[36] A. Stern, T. Scaffidi, O. Reuven, C. Kumar, J. Birkbeck, and S. Ilani, Phys. Rev. Lett. **129**, 157701 (2022).

[37] O. E. Raichev, Phys. Rev. B **106**, 085302 (2022).

[38] B. N. Narozhny, Ann. Phys. (Amsterdam) **411**, 167979 (2019).

[39] B. N. Narozhny, I. V. Gornyi, M. Titov, M. Schütt, and A. D. Mirlin, Phys. Rev. B **91**, 035414 (2015).

[40] G. Y. Vasileva, D. Smirnov, Y. L. Ivanov, Y. B. Vasilyev, P. S. Alekseev, A. P. Dmitriev, I. V. Gornyi, V. Y. Kachorovskii, M.

Titov, B. N. Narozhny, and R. J. Haug, Phys. Rev. B **93**, 195430 (2016).

[41] A. B. Kashuba, Phys. Rev. B **78**, 085415 (2008).

[42] M. Müller and S. Sachdev, Phys. Rev. B **78**, 115419 (2008).

[43] M. S. Foster and I. L. Aleiner, Phys. Rev. B **79**, 085415 (2009).

[44] M. Schütt, P. M. Ostrovsky, I. V. Gornyi, and A. D. Mirlin, Phys. Rev. B **83**, 155441 (2011).

[45] U. Briskot, M. Schütt, I. V. Gornyi, M. Titov, B. N. Narozhny, and A. D. Mirlin, Phys. Rev. B **92**, 115426 (2015).

[46] J. M. Link, B. N. Narozhny, E. I. Kiselev, and J. Schmalian, Phys. Rev. Lett. **120**, 196801 (2018).

[47] B. N. Narozhny, I. V. Gornyi, and M. Titov, Phys. Rev. B **104**, 075443 (2021).

[48] M. P. Marder, *Condensed Matter Physics* (Wiley, New York, 2010).

[49] B. N. Narozhny and I. V. Gornyi, Front. Phys. **9**, 640649 (2021).

[50] M. Müller, J. Schmalian, and L. Fritz, Phys. Rev. Lett. **103**, 025301 (2009).

[51] B. N. Narozhny, I. V. Gornyi, and M. Titov, Phys. Rev. B **103**, 115402 (2021).

[52] See Supplemental Material at http://link.aps.org/supplemental/10.1103/PhysRevB.107.045413 for technical details.

[53] M. Kamada, V. Gall, J. Sarkar, M. Kumar, A. Laitinen, I. Gornyi, and P. Hakonen, Phys. Rev. B **104**, 115432 (2021).

[54] M. Kumar, A. Laitinen, and P. Hakonen, Nat. Commun. **9**, 2776 (2018).

[55] B. L. Altshuler and A. G. Aronov, in *Electron-Electron Interactions in Disordered Systems*, edited by A. L. Efros and M. Pollak (North-Holland, Amsterdam, 1985).

[56] G. Zala, B. N. Narozhny, and I. L. Aleiner, Phys. Rev. B **64**, 214204 (2001).

[57] L. D. Landau and E. M. Lifshitz, *Fluid Mechanics* (Pergamon, London, 1987).

[58] B. N. Narozhny, I. L. Aleiner, and A. Stern, Phys. Rev. Lett. **86**, 3610 (2001).

[59] I. S. Burmistrov, M. Goldstein, M. Kot, V. D. Kurilovich, and P. D. Kurilovich, Phys. Rev. Lett. **123**, 026804 (2019).

[60] D. Halbertal, J. Cuppens, M. Ben Shalom, L. Embon, N. Shadmi, Y. Anahory, H. R. Naren, J. Sarkar, A. Uri, Y. Ronen, Y. Myasoedov, L. S. Levitov, E. Joselevich, A. K. Geim, and E. Zeldov, Nature (London) **539**, 407 (2016).

[61] D. Halbertal, M. Ben Shalom, A. Uri, K. Bagani, A. Y. Meltzer, I. Markus, Y. Myasoedov, J. Birkbeck, L. S. Levitov, A. K. Geim, and E. Zeldov, Science **358**, 1303 (2017).

[62] A. Aharon-Steinberg, A. Marguerite, D. J. Perello, K. Bagani, T. Holder, Y. Myasoedov, L. S. Levitov, A. K. Geim, and E. Zeldov, Nature (London) **593**, 528 (2021).

[63] L. Ella, A. Rozen, J. Birkbeck, M. Ben-Shalom, D. Perello, J. Zultak, T. Taniguchi, K. Watanabe, A. K. Geim, S. Ilani, and J. A. Sulpizio, Nat. Nanotechnol. **14**, 480 (2019).